Ionization of Nitric Acid on Ice

Christopher J. Pursell,* Michael A. Everest, Mary E. Falgout, and Diana D. Sanchez

Department of Chemistry, Trinity University, 715 Stadium Drive, San Antonio, Texas 78212-7200

Received: February 27, 2002; In Final Form: June 10, 2002

The ionization of nitric acid on the surface of crystalline ice was examined from 130 to 150 K using FTIR transmission spectroscopy. A spectral feature of the hydronium ion, H_3O^+, was monitored as a function of time. The results are best understood when they are separated into (a) low and (b) high nitric acid exposure, depending upon the amount of nitric acid adsorbed on the ice surface. (a) For low nitric acid exposure (($\sim$2−20) $\times$ 10^{15} molecules/cm^2), the absorbance of H_3O^+ can be fit to a single exponential (i.e., first-order expression). The resulting rate constant, $k = (4.9 \pm 0.7) \times 10^{-3}$ s^{-1}, is attributed to the dissolution of the ions in the ice surface layer (i.e., a reactive layer on the ice surface). The thickness of this ice surface layer is estimated to be 10 nm. (b) For high nitric acid exposure (($\sim$20−200) $\times$ 10^{15} molecules/cm^2), the absorbance of H_3O^+ can be fit to a double exponential expression that is composed of the first-order rate constant above, along with another first-order rate constant, $k' = (5.2 \pm 0.7) \times 10^{-4}$ s^{-1}. This rate constant is attributed to the dissolution of ions in an acid-rich ice surface layer. Both rate constants are independent of temperature, indicating a small activation energy ($E_a = 0 \pm 2$ kcal/mol).

Introduction

The interaction of molecular species with the surface of ice continues to be of importance in many areas of science. For example, the heterogeneous chemistry in the polar stratosphere that leads to ozone destruction over Antarctica every spring continues to be an area of intense research.[1−3] Though much experimental work has been performed in an effort to better understand these types of reactions, there remains much to be learned. One important aspect that interests us concerns the role of water on the surface of ice. In particular, if these reactions are ionic, what role does the surface water play in hydrating the ions? Is there a limit to the number of ionic species that can be accommodated on the surface?

Our research group has therefore been examining chemical reactions in ice and on ice surfaces.[4−7] In the laboratory, we use thin films of pure water ice and examine the interaction of reactive gases with the ice surface using infrared transmission spectroscopy. Our most recent study[4] examined the reactivity difference between the surface and the bulk of H_2O ice by monitoring the isotope exchange of D_2O. Interestingly, no exchange occurs on the surface of ice but does occur in bulk ice. The surface became reactive only after the ice was doped with a small amount of acid, suggesting a depletion of mobile defects or protons on the surface of neutral ice. Additionally, our study[5] of the acid−base reaction HCl + NH_3 on crystalline ice suggested that the availability of water on the surface affects the chemistry. The formation of the ammonium ion, NH_4^+, was limited below 140 K but became the dominant species above this temperature. This change in chemistry was attributed to the greater number of water molecules on the ice surface that are available for hydration.

In this report, we present results for the ionization of nitric acid on crystalline ice. Whereas previous studies of the interaction of nitric acid with ice are numerous (see, for example, refs 8−14), this report is the first kinetics study of the ionization of the acid on ice. We examined the ionization kinetics using FTIR transmission spectroscopy to monitor the formation of the hydronium ion, H_3O^+, as a function of time. Whereas these studies were performed over a temperature range that is lower than that found in the stratosphere, the results are helpful in our continued efforts to better understand chemistry on ice in general.

Experimental Section

The experimental apparatus has been described previously.[4,5] Briefly, a liquid nitrogen-cooled cryostat or closed-cycle helium refrigerator cryostat cooled an infrared transparent window (ZnSe) that was attached to the coldfinger. The cryostat is static and was not pumped on during an experiment. However, cryopumping of condensable gases in the cryostat vacuum by the liquid nitrogen reservoir or the helium coldfinger reduced the pressure to 10^{-6}−10^{-7} Torr, which is predominantly residual nitrogen and oxygen. Mass spectrum analysis of residual gases (i.e., water and nitric acid during an experiment) indicate partial pressures $<10^{-8}$ Torr. The cryostat sat inside the sample compartment of a commercial FTIR spectrometer such that transmission was measured. All infrared spectra were collected with 4-cm^{-1} resolution and 32 scans each, which gave a collection time of $\sim$40 s. The time resolution was therefore about 40 s. The temperature was measured with a silicon diode and was controlled to better than 0.2 K. A vacuum manifold equipped with a heated capacitance manometer, a liquid nitrogen trap, a diffusion pump, and a mechanical pump was used for gas-sample handling. Gases (H_2O and HNO_3), transferred to the cryostat using a variable leak valve, were directed at the ZnSe window, and an effusive beam exposed one side of the window.

Experiments were performed in the following manner. A thin film of crystalline ice (ca. 0.3 μm)[15] was formed by spray deposition of water vapor onto the ZnSe window held at 150 K. The temperature was then adjusted to the temperature of interest, and the ice was allowed to stabilize for about 30 min.

* Corresponding author. E-mail: Cpursell@trinity.edu.

10.1021/jp025697k CCC: $22.00
Published on Web 07/26/2002

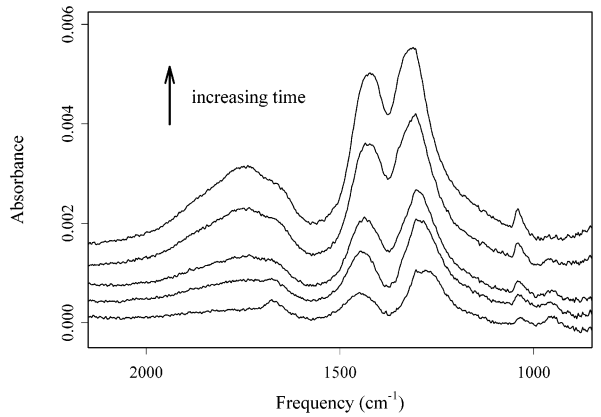

Figure 1. Representative infrared difference spectra of the ionization of nitric acid on crystalline ice for low acid exposure corresponding to a surface coverage of 8×10^{15} molecules/cm^2. Spectra were collected at 145 K for 90 min.

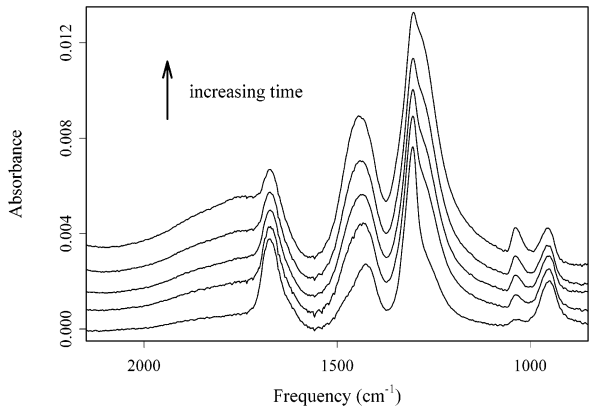

Figure 2. Representative infrared difference spectra of the ionization of nitric acid on crystalline ice for high exposure corresponding to a surface coverage of 100×10^{15} molecules/cm^2. Spectra were collected at 145 K for 90 min.

A background spectrum of the crystalline ice was collected. The variable leak valve was quickly opened, and HNO_3 vapors were sprayed onto the ice film. As soon as the leak valve was closed, infrared "difference" spectra (i.e., (ice + nitric acid) − ice) were collected every 8 s (only 4 scans) as the reaction initially proceeded and as residual acid vapors effused to the ice surface. A plot of the peak height for a molecular nitric acid feature at 954 cm^{-1} suggests that nearly all the nitric acid has reached the ice surface 30−60 s after closing the leak valve. Any excess nitric acid and water vapors are continually cryopumped away by the liquid nitrogen reservoir or the helium-cooled coldfinger. There is no evidence of slow vapor transfer from the cryostat's walls. After about 30 s, spectra were collected every 40 s (32 scans) until the reaction appeared to slow, at which point spectra were collected at longer time intervals (but still 32 scans). Experiments were performed every 5 K between 130 and 150 K. Nearly 30 experiments were performed, with at least three experiments at each temperature.

The amount of nitric acid transferred to the ice surface was determined in a manner similar to that reported previously.[4,5] In particular, the amount of nitric acid was based upon a calibration of the average pressure drop of nitric acid in the gas-handling manifold. Using a sticking or uptake coefficient of $\gamma = 0.3$,[8] this led to an average surface coverage of 10×10^{15} molecules/cm^2. (Residual nitric acid vapor is cryopumped to colder surfaces.) Using this calibration of the pressure drop in the gas manifold, the experimental surface coverage of nitric acid was effectively varied from $(2-200) \times 10^{15}$ molecules/cm^2. As explained below, the results are best understood when they are separated into two ranges: (a) a low-exposure range of $\sim(2-20) \times 10^{15}$ molecules/cm^2 and (b) a high-exposure range of $\sim(20-200) \times 10^{15}$ molecules/cm^2.

Results

Infrared transmission spectra for the ionization of nitric acid on ice are presented in Figures 1 (low exposure) and 2 (high exposure). These infrared difference spectra were collected as a function of time after the crystalline ice was exposed to a small amount of nitric acid vapor (ca. 8×10^{15} and 100×10^{15} molecules/cm^2, respectively).

Analysis of the infrared spectra resulting from the interaction of nitric acid with crystalline ice between 130 and 150 K is based upon a comparison of the previously observed infrared spectra of the amorphous hydrates of nitric acid, namely, nitric acid monohydrate (NAM) and nitric acid trihydrate (NAT).

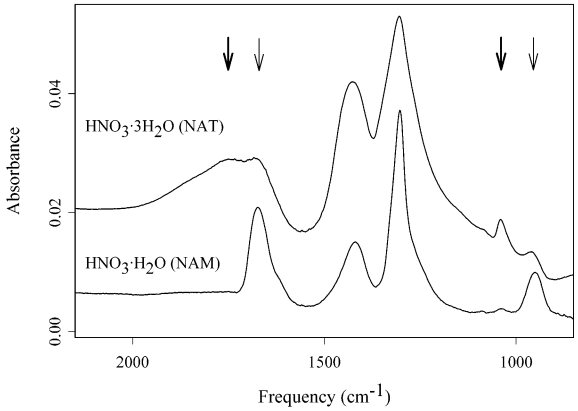

Figure 3. Reference infrared spectra of thin films (ca. 0.1 μm) of *amorphous* hydrates of nitric acid collected in the range 130−150 K. Identification is based upon refs 16 and 17. Important spectral features for molecular HNO_3 are at 954 and 1670 cm^{-1} (thin arrows); for NO_3^-, at 1040 cm^{-1}; and for H_3O^+, at 1750 cm^{-1} (thick arrows). Comparing NAM to NAT, the intensity of the H_3O^+ band at 1750 cm^{-1} increases whereas the molecular nitric acid peak at 1670 cm^{-1} decreases, indicating an increase in the extent of ionization.

Reference infrared spectra are displayed in Figure 3. The infrared identification of these species was first reported by Devlin[16] and later confirmed by Tolbert.[17] Important spectral features are (1) molecular HNO_3 at 954 and 1670 cm^{-1}, (2) NO_3^- at 1040 cm^{-1}, and (3) H_3O^+ at 1750 cm^{-1}.[16] (The nitrate bands between 1200 and 1400 cm^{-1} are not as informative.) Examination of the relative intensities of these peaks in Figure 3, especially the H_3O^+ peak at 1750 cm^{-1}, indicates that the extent of ionization of the acid in these amorphous hydrates is greater in NAT than in NAM.[16,18]

Comparisons of Figures 1 and 2 with Figure 3 indicate that when the nitric acid vapor is initially adsorbed on the ice surface it produces a difference spectrum resembling the spectrum of amorphous nitric acid monohydrate (NAM). The nitric acid is therefore mostly molecular. As the spectra evolve in time, they appear to resemble the spectrum of the mostly ionic, amorphous nitric acid trihydrate (NAT). The unique hydronium peak at 1750 cm^{-1} is indicative of the ionization of the acid. For our experimental conditions ($T = 130-150$ K, $P_{water} < 10^{-8}$ Torr, $P_{nitric\ acid} < 10^{-8}$ Torr), NAT should be the thermodynamically stable phase.[19]

The ionization of nitric acid as a function of time was therefore monitored by measuring the amount of H_3O^+ formed using the band centered at 1750 cm^{-1}. The peak height at 1786

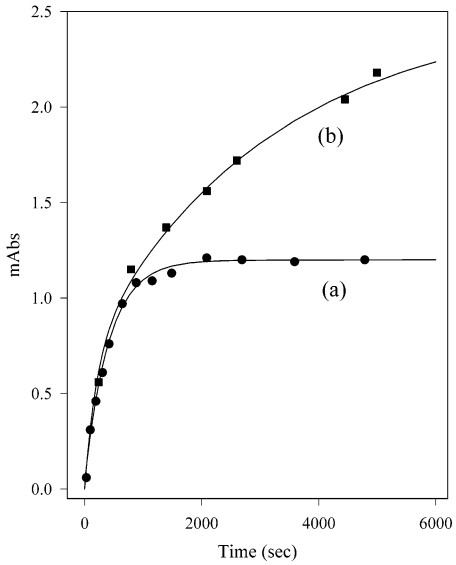

Figure 4. Representative kinetics plot of the infrared intensity of the H_3O^+ band measured at 1786 cm^{-1} as a function of time. (a) Single-exponential, first-order fit to the low-exposure data from Figure 1, according to eq 1. (b) Double exponential fit to the high-exposure data from Figure 2, according to eq 2.

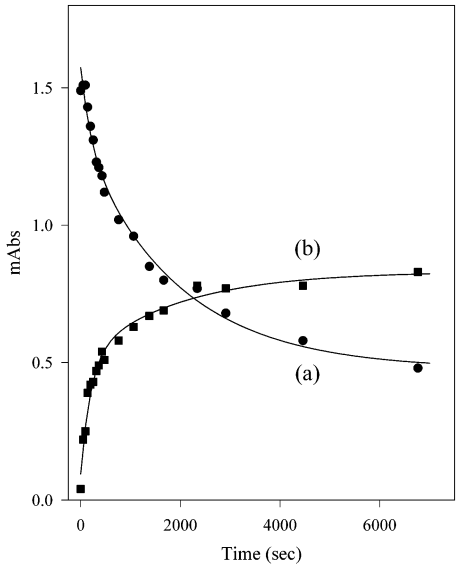

Figure 5. Representative kinetics plot of the infrared intensity of (a) the molecular HNO_3 band at 954 cm^{-1} and (b) the ionic NO_3^- band at 1040 cm^{-1} as a function of time. The experimental conditions are similar to those of Figure 2 for high exposure. A double-exponential fit to the data is shown using the rate constants determined from eq 2, namely, $k = 4.9 \times 10^{-3}$ s^{-1} and $k' = 5.2 \times 10^{-4}$ s^{-1}.

cm^{-1} was actually used after determining that the peak height and integrated area produced the same results within the experimental uncertainty. This peak position was chosen as a compromise: it was over 100 cm^{-1} from the molecular nitric acid peak at 1670 cm^{-1} and yet was near the maximum height at 1750 cm^{-1}. Representative plots of the absorbance height of this H_3O^+ peak as a function of time are presented in Figure 4. The data presented are for the infrared spectra displayed in Figures 1 and 2 for low and high acid exposure, respectively. Figure 4 illustrates that the results can be separated into two ranges, low and high nitric acid exposure. As discussed below, the low-exposure results can be fit very well by a single exponential, whereas the high-exposure results require a double exponential.

The ionization could also be monitored by following the loss of molecular HNO_3 at 954 cm^{-1} and the formation of ionic NO_3^- at 1040 cm^{-1}. A representative plot of these two peaks is shown in Figure 5. The rate constants for the fits are the same as those in Figure 4, as discussed below. For the very lowest exposure experiments, these peaks were very close to the noise level and were difficult to analyze. Additionally, the large nitrate peaks in the 1200−1400 cm^{-1} region cause curvature in the baseline, creating additional difficulties in measuring the peak heights. Because these plots yielded the same rate constants as those from plots of the H_3O^+ peak at 1786 cm^{-1}, which consistently produced better signal levels, we analyzed this peak. When the molecular HNO_3 peak at 954 cm^{-1} and the ionic NO_3^- peak at 1040 cm^{-1} could be analyzed, they could consistently be fit using the rate constants from the analysis of the ionic H_3O^+ peak at 1786 cm^{-1}.

For low nitric acid exposure ($\sim(2-20) \times 10^{15}$ molecules/cm^2), the absorbance data was fit to a single-exponential, first-order expression

$$A(t) = A_\infty(1 - e^{-kt}) \qquad (1)$$

where k is a first-order rate constant and A_∞ is the asymptotic limit. This limit corresponds to the maximum amount of H_3O^+ formed and is therefore a measure of the extent of the reaction at completion on the surface. A typical fit is included in Figure 4. Consistent with a first-order process, the rate constant is also independent of the amount of nitric acid over the range $\sim(2-20) \times 10^{15}$ molecules/cm^2. The average first-order rate constant for all measurements is $k = (4.9 \pm 0.7) \times 10^{-3}$ s^{-1} (all reported uncertainties are the 90% confidence interval). Over the small temperature range 130−150 K, the rate constant is independent of temperature. An Arrhenius plot yields an energy barrier of $E_a = 0 \pm 2$ kcal/mol. The extent of reaction, as determined by the asymptotic limit at long times of the amount of H_3O^+ formed (i.e., A_∞ in eq 1 above), also appears to be independent of both temperature and the amount of nitric acid added (over the range $\sim(2-20) \times 10^{15}$ molecules/cm^2). The average extent of ionization for all measurements is $A_\infty = 0.70 \pm 0.11$ mAbs.

For high nitric acid exposure ($\sim(20-200) \times 10^{15}$ molecules/cm^2), the data was fit to the following double exponential expression:

$$A(t) = A_\infty(1 - e^{-kt}) + B(1 - e^{-k't}) \qquad (2)$$

k and A_∞ were fixed to the values established by the low-exposure studies, k' is a first-order rate constant, and B is a fitting constant. A typical fit is shown in Figure 4. The average value of this rate constant is $k' = (5.2 \pm 0.7) \times 10^{-4}$ s^{-1}, which is also temperature-independent over the temperature range studied, with an energy barrier of $E_a = 0 \pm 2$ kcal/mol. The constant B varied with the amount of nitric acid exposure.

Justification for fitting the absorbance data as outlined above comes from multiple exposure experiments. For these experiments, low-exposure nitric acid interacted with an ice surface producing spectra identical to Figure 1, which was fit according to eq 1. After the absorbance due to H_3O^+ stopped changing, reaching its asymptotic limit A_∞, the ice surface was exposed to additional nitric acid. The resulting spectra resembled the later time spectra in Figure 2 (for high exposure) and could be fit to the single-exponential expression

$$A(t) = B(1 - e^{-k't}) \qquad (3)$$

where k' has the same value as in eq 2 for high-exposure and B varied with the amount of nitric acid exposure.

Discussion

The ionization of nitric acid on ice can be explained by the following two-step mechanism

$$(1)\ HNO_3(g) + H_2O(s) \rightarrow HNO_3{\cdot}H_2O\ (ad)$$

$$(2)\ HNO_3{\cdot}H_2O(ad) \xrightarrow{k,\,k'} NO_3^-(solv) + H_3O^+(solv)$$

where g, s, ad, and solv denote gas, surface, adsorbed, and solvated, respectively. Step 1 is very fast and represents the initial adsorption of the acid by the ice, which occurs within the first 60 s of closing the leak valve for the nitric acid vapor. The acid is initially adsorbed as a covalent unit prior to engaging in proton transfer and hydration, similar to that of the HCl acid.[20−22] Once adsorbed, the acid employs its strength as a proton donor to disrupt the hydrogen bonds of the ice surface, similar to the process with HCl.[23] The acid in then able to penetrate the surface and ionize as it is embedded in the ice surface layer (i.e., a reactive layer on the ice). Step 2 represents this ionization of the acid and subsequent separation or dissolution of the ions in the ice surface layer. *Our observed first-order kinetics corresponds to this slower second step.*

For low exposure, the kinetics of dissolution of the ions, NO_3^- and H_3O^+, should be related to their diffusion in the ice surface layer. Whereas the diffusion of H_3O^+ would be very fast because it occurs by proton hopping,[24] the diffusion of NO_3^- would be slower and rate-limiting. The NO_3^- diffusion in the ice surface layer should be comparable to the measured diffusion of HNO_3 in ice.[25] Our experimentally determined first-order rate constant should therefore be similar to the average diffusion time of nitric acid in ice. In other words, $k \approx 1/\tau$, where τ is the average time for diffusion according to

$$\tau = \delta^2/(2D_o) \qquad (4)$$

Assuming an average distance $\delta = 1-2$ bilayers of water (ca. 0.36−0.73 nm) and using a diffusion coefficient $D_o = 5.45 \times 10^{-18}$ cm^2/s (extrapolated to 150 K),[25] the calculated rate constant is $1/\tau = (2-8) \times 10^{-3}$ s^{-1}, which agrees with our experimental value of $k = (4.9 \pm 0.7) \times 10^{-3}$ s^{-1}. For high nitric acid exposure, the dissolution would be into a nitric acid-rich ice surface layer. One would suspect that this diffusion is even slower, and a factor of 10 is not unreasonable.[26]

The apparent temperature independence of this dissolution step indicates a small activation barrier, $E_a = 0 \pm 2$ kcal/mol. For this mechanism, one would expect a barrier closer to that for the breaking of a hydrogen bond in ice, ca. 8−12 kcal/mol. However, the localized heat released during the solvation of the ions might compensate for the breaking of the H-bonds, yielding a very low, experimentally observed energy barrier.

At first glance, this mechanism does not agree with the observation that the extent of ionization, the maximum amount of H_3O^+ formed at completion, is independent of the amount of nitric acid adsorbed (for the low exposure range of ∼(2−20) × 10^{15} molecules/cm^2). More HNO_3 should produce more H_3O^+. However, if the adsorption of nitric acid according to the first step is limited by the availability of water on the surface of ice, then only a limited amount of $HNO_3{\cdot}H_2O$ can be formed in the surface layer. This limited amount would be ionized according to step 2 with the rate constant k to produce a limited amount of H_3O^+. For high nitric acid exposure, only a limited amount of the initial nitric acid forms $HNO_3{\cdot}H_2O$ at the ice interface and reacts according to k to produce a maximum amount A_∞ of H_3O^+, whereas the excess acid must react according to the slower rate constant k'. It should be noted that the transition from low to high exposure is not sharp. Around 20×10^{15} molecules/cm^2, the data cannot be fit to a single exponential but require a double exponential.

This mechanism suggests that the ionization of the nitric acid on ice is limited by the availability of water at the surface, which would be consistent with our previous studies.[4,5] Under the conditions of these experiments, only a limited amount of acid can be adsorbed at the ice surface. Extra acid is prevented or slowed from penetrating this layer, which acts like a protective crust[27] on the ice. Assuming that all the nitric acid adsorbed in this surface layer reacts and forms a uniform layer of NAT, we can estimate the thickness of this reactive layer. On the basis of other studies in our laboratory involving spectroscopic conversion factors for the thickness of NAT films along with work from Tolbert,[9] the average extent of 0.70 mAbs at 1786 cm^{-1} corresponds to a thickness of 10 nm. (Using a density for NAT of 1.5 g/cm^3,[28] a thickness of 10 nm gives a surface coverage of 8×10^{15} molecules/cm^2, which agrees with our experimental surface coverages of ∼(2−20) × 10^{15} molecules/cm^2.) Tolbert and Middlebrook[9] discovered similar results at 183 K. They exposed thick ice films (ca. 1.1 μm) to 1.8×10^{-6} Torr of nitric acid, which formed a thin layer of *crystalline* NAT. The surface reached a saturation limit, similar to our maximum extent of reaction, corresponding to a NAT thickness of 22 nm.

Conclusions

The ionization of nitric acid on the surface of crystalline ice was examined from 130 to 150 K using FTIR transmission spectroscopy. A spectral feature of the hydronium ion, H_3O^+, was monitored as a function of time. The ionization follows simple first-order kinetics. The results are separated into low and high nitric acid exposure, depending upon the amount of nitric acid adsorbed on the ice surface. For low nitric acid exposure, the absorbance of H_3O^+ was fit to a single first-order expression. The resulting rate constant, $k = (4.9 \pm 0.7) \times 10^{-3}$ s^{-1}, is attributed to the dissolution of the ions in the ice surface layer. This dissolution rate constant agrees with previously measured diffusion coefficients for HNO_3 in ice. For high nitric acid exposure, the absorbance of H_3O^+ was fit to a double exponential expression that is composed of the first-order rate constant above, along with another first-order rate constant, $k' = (5.2 \pm 0.7) \times 10^{-4}$ s^{-1}. This additional rate constant, being an order of magnitude smaller than the rate constant for low nitric acid exposure, is attributed to the dissolution of ions in an acid-rich ice surface layer. Both rate constants are independent of temperature, indicating a small activation energy. The maximum amount of H_3O^+ formed on the surface (i.e., the asymptotic limit at long times) is also independent of both temperature and the amount of nitric acid added to the ice surface. Assuming that all the nitric acid that forms the maximum amount of H_3O^+ is NAT, the reactive surface layer on ice is estimated to be 10 nm thick.

Although these studies were performed at temperatures lower than those found in the atmosphere, we believe that they provide some insight into the importance of understanding the nature of the ice surface and its role in hydrating ionic species. The present results, along with our earlier results,[4,5] suggest that there is a limited amount of water available on the ice surface that can participate in hydration and heterogeneous chemistry. Very similar conclusions have been reported recently by Devlin et

al.[22] They state that "the surface of crystalline ice is one of limited availability of water of hydration".[22] Their results for the evolution of nitric acid on nanocrystals of ice are also qualitatively very similar to our results presented above. This surface water layer can be thought of as a thin reactive layer on the ice surface and may be consistent with the quasi-liquidlike layer on ice proposed by Molina.[29] Furthermore, in the case of nitric acid, the formation of a thin hydrate layer on the ice surface may act as a crust that limits additional uptake because subsequent nitric acid would have to diffuse through the hydrate crust.[27]

Acknowledgment. Our studies have been motivated by interactions with many researchers in the field and the growing body of literature regarding atmospheric heterogeneous chemistry. We are especially indebted to the published work from Dr. Tolbert's group at the University of Colorado and Dr. Devlin's group at Oklahoma State University. We have also benefited greatly from discussions with Dr. Devlin concerning the nature of the ice surface. This work has been financially supported by Trinity University, the Dreyfus Foundation, the Research Corporation, the donors of the Petroleum Research Fund, and the Welch Foundation.

References and Notes

(1) Solomon, S.; Garcia, R. R.; Rowland, F. S.; Wuebbles, D. J. *Nature (London)* **1986**, *321*, 755.

(2) Cicerone, R. J. *Science (Washington, D.C.)* **1987**, *237*, 35.

(3) Solomon, S. *Rev. Geophys.* **1988**, *26*, 131. World Meteorological Organization (WMO). *Scientific Assessment of Stratospheric Ozone: 1989*; Report No. 20; WMO: Geneva, 1990.

(4) Everest, M. A.; Pursell, C. J. *J. Chem. Phys.* **2001**, *115*, 9843.

(5) Pursell, C. J.; Zaidi, M.; Thompson, A.; Fraser-Gaston, C.; Vela, E. *J. Phys. Chem. A* **2000**, *104*, 552.

(6) Pursell, C. J.; Conyers, J.; Denison, C. *J. Phys. Chem.* **1996**, *100*, 15450.

(7) Pursell, C. J.; Conyers, J.; Alapat, P.; Parveen, R. *J. Phys. Chem.* **1995**, *99*, 10433.

(8) Leu, M.-T. *Geophys. Res. Lett.* **1988**, *15*, 17.

(9) Tolbert, M. A.; Middlebrook, A. M. *J. Geophys. Res.* **1990**, *95*, 22423.

(10) Hanson, D. R. *Geophys. Res. Lett.* **1992**, *19*, 2063.

(11) Laird, S. K.; Sommerfeld, R. A. *Geophys. Res. Lett.* **1995**, *22*, 921.

(12) Zondlo, M. A.; Barone, S. B.; Tolbert, M. A. *Geophys. Res. Lett.* **1997**, *24*, 1391.

(13) Abbatt, J. P. D. *Geophys. Res. Lett.* **1997**, *24*, 1479.

(14) Arora, O. P.; Cziczo, D. J.; Morgan, A. M.; Abbatt, J. P. D.; Niedziela, R. F. *Geophys. Res. Lett.* **1999**, *26*, 3621.

(15) The ice film's thickness was determined using the IR absorbance at 820 cm^{-1} along with a Beer's law-like conversion factor (1 $\mu m = 0.163$ Abs at 820 cm^{-1}) from the literature (see refs 5 and 9).

(16) Ritzhaupt, G.; Devlin, J. P. *J. Phys. Chem.* **1991**, *95*, 90.

(17) Koehler, B. G.; Middlebrook, A. M.; Tolbert, M. A. *J. Geophys. Res.* **1992**, *97*, 8065.

(18) Barton, N.; Rowland, B.; Devlin, J. P. *J. Phys. Chem.* **1993**, *97*, 5848.

(19) Hanson, D. R.; Mauersberger, K. *Geophys. Res. Lett.* **1988**, *15*, 855.

(20) Robertson, S. H.; Clary, D. C. *Faraday Discuss.* **1995**, *100*, 309.

(21) Clary, D. C.; Wang, L. *J. Chem. Soc., Faraday Trans.* **1997**, *93*, 2763.

(22) Devlin, J. P.; Uras, N.; Rahman, M.; Buch, V. *Isr. J. Chem.* **1999**, *39*, 261.

(23) Delzeit, L.; Powell, K.; Uras, N.; Devlin, J. P. *J. Phys. Chem. B* **1997**, *101*, 2327.

(24) Hobbs, P. V. *Ice Physics*; Clarendon Press: Oxford, 1974.

(25) Thibert, E.; Domine, F. *J Phys. Chem. B* **1998**, *102*, 4432.

(26) The diffusion of HDO was measured to be 30−70 times slower in nitric acid-dosed ice relative that in to pure ice. Livingston, F. E.; George, S. M. *J Phys. Chem. B* **1999**, *103*, 4366.

(27) Uras, N.; Devlin, J. P. *J. Phys. Chem. A* **2000**, *104*, 5770.

(28) Sohnel, O.; Novotny, P. *Densities of Aqueous Solutions of Inorganic Substances*; Elsevier: Amsterdam, 1985.

(29) Molina, M. J. In *Chemrawn VII: Chemistry of the Atmosphere: The Impact of Global Change*; Calvert, J. G., Ed.; Blackwell Scientific Publishers: Oxford, 1993.